Journal of the European Ceramic Society 39 (2019) 1287–1296

Contents lists available at ScienceDirect

Journal of the European Ceramic Society

journal homepage: www.elsevier.com/locate/jeurceramsoc

Original Article

Comparison of low and high pressure infiltration regimes on the density and highly porous microstructure of ceria ecoceramics made from sustainable cork templates

Rui M. Novais*, Robert C. Pullar

Department of Materials and Ceramic Engineering / CICECO- Aveiro Institute of Materials, University of Aveiro, Campus Universitário de Santiago, 3810-193, Aveiro, Portugal

ARTICLE INFO

Keywords:
Cork
Ecoceramics
Ceria
Biomorphic
Porous

ABSTRACT

Cork templates were used to produce lightweight bulk biomimetic ecoceramic (environmentally conscious ceramic) monoliths. Bulk/monolithic ceramics are vital for many applications, i.e. energy materials and fuel cells. Using simple and flexible, aqueous green-chemistry procedures, for the first time the influence of infiltration regime, number of infiltration cycles and sintering temperature on ecoceramic density and microstructure was studied. This lightweight three-dimensionally ordered macroporous (3DOM) CeO_2 preserved the hexagonal cellular structure of cork, but unlike the wood, the rear cell walls were open, greatly increasing open porosity. Higher sintering temperatures (1600 instead of 1000 °C) were required to produce cm size monolithic ecoceramics mechanically strong enough to be handled. The infiltration regime and number of infiltration cycles affected density and porosity. Lower infiltration pressure led to higher porosity ecoceramics (3.3–5.7%), which may favour catalytic performance, showing the possibility of tailoring porosity and specific surface area by modifying the number of infiltration cycles.

1. Introduction

The production of biomorphic ceramics using renewable/sustainable natural resources, also known as ecoceramics (environmentally conscious ceramics) [1,2], is an exciting approach to fabricate materials exhibiting complex structures and functionalities. Moreover, their low cost of production and the possibility of using a wide variety of precursors with unique microstructures explains the increasing attention provided to these materials. Natural and renewable materials such as wood and wood wastes, vegetable fibres and sawdust have been considered for the manufacture of ecoceramics. In fact, several types of wood (hard and soft) have been used as a template for the production of this new class of materials, including pine [3], platane [4], bamboo [5], beech [6], poplar [7], balsa, maple and oak [8] precursors have been investigated. In all cases, the wood template is first pyrolysed to form a pure carbon skeleton which maintains the microstructure, but which can be impregnated with a precursor liquid or gas. The first such "ceramic wood" to be made was SiC [9], and since then the vast majority of research has been into non-oxide ecoceramics such as carbides and nitrides, with investigations of a few oxides such as Al_2O_3 [10], ZrO_2 [2] and ferrites [11].

Although most woods have a density below one, often of around 0.4-0.8 g/cm^3 [12], few are highly porous and lightweight, and of the woods used for ecoceramics only balsa (0.16 g/cm^3) can compare to the low density of cork (which can be as low as 0.12 g/cm^3), as even pine and bamboo are several times more dense than cork. However, despite this, cork has never been used to make ecoceramics until the work of Pullar et al. [13,14] who reported the creation of magnetic hexagonal ferrite ecoceramics made from cork in 2015. Since then, only three works addressing cork-based ecoceramics have been reported: one on non-oxide SiC [15] in 2016, and two other by the authors on ceria produced from waste cork sawdust [16] and cork granules (mm size) [17] in 2016 and 2018, respectively. Here we report the production of monolithic CeO_2 ecoceramics (cm size) by using bulk cork samples (wine stoppers) as template. This is the first ever report addressing the influence of the infiltration technique, sintering temperature and number of infiltration cycles on the ceria ecoceramics' density and microstructure. This investigation decreases the existing knowledge gap regarding the synthesis and most influential factors affecting the production of monolithic size ceria ecoceramics.

Cork is the bark of an evergreen oak tree (*Quercus suber L.*) native to a few countries around the Mediterranean basin. Worldwide, cork oak

* Corresponding author.
E-mail address: ruimnovais@ua.pt (R.M. Novais).

https://doi.org/10.1016/j.jeurceramsoc.2018.11.050
Received 27 September 2018; Received in revised form 26 November 2018; Accepted 30 November 2018
Available online 01 December 2018

forests occupy 2.1 million hectares of land, 34% being located in Portugal, which represents 23% of the Portuguese national forest [18]. Portugal is the world's largest cork producer [19], supplying around 50% [18]. Cork is harvested from the tree regularly every 9 years [20], without damaging the tree, which has an active productive life of at least 200 years, and many live even longer. This is an exceptional renewable resource, since the cork layer is regenerated after each extraction, and will absorb the equivalent amount of CO_2 which may be released from the cork during processing. Moreover, cork extraction actually increases the CO_2 absorption of the tree during its lifetime by up to five times, in order to regenerate the bark [21], and as such cork is a uniquely sustainable material, sequestering up to 5.7 T CO_2/ha/yr [22]. Furthermore, cork forests are one of the best examples of balanced conservation and development anywhere in the world, playing a key role in ecological processes such as water retention, soil conservation and carbon storage. The cork oak forests of Portugal are also considered to be "Europe's Amazonian forests", supporting the greatest degree of bio-diversity anywhere in Europe, with up to 135 plant species per m^2 [22].

Cork has a microstructure different to other lignocellulosic woods, consisting of hollow polyhedral cells, with a hexagonal honeycomb shape (~20 μm diameter) when viewed from the radial direction coming out of the tree, and a rectangular shape (~45 μm length, resembling a brick wall) when viewed from the transverse side or top directions [22,23]. There are up to 200 million cells per cm^3 [24], and due to this structure, cork exhibits exceptional thermal, acoustic and vibrational insulation, and a very low density of 0.12-0.24 g/cm^3 [25], the higher densities occurring when the cell walls are corrugated. Therefore, it is an ideal natural template to form ecoceramics, although in natural cork all the cells are sealed with front and rear walls, and as such it has a low open porosity and is not very permeable.

Cerium oxide (CeO_2) has long being recognised as an exciting material due to its excellent redox properties [26] and oxygen storage / release capacity [27]. It has a wide range of applications, such as electrolytes for solid fuel cells [28], microwave and THz dielectric materials [29], and as an UV absorber [30]. Recently, the possibility of using CeO_2 for thermochemical fuel production (TCFP) [31,32], for example to split water and produce hydrogen, has further boosted the interest in this exceptional material. The synthesis of three-dimensionally ordered macroporous (3DOM) CeO_2 could be advantageous for these applications. In this context, cork emerges as an outstanding natural template for the production of 3DOM CeO_2 due to its regular 3DOM structure, consisting of hollow hexagonal honeycomb cells [23].

Up to now there have been very few investigations into CeO_2 ecoceramics [16,33]. In 2008, Matovic et al. [33] reported the production of porous $Ce_{1-x}Gd_xO_{2-\delta}$ using Linden (*Tilia amurensis*) wood as a template. However, the fabrication process involved acid or alkaline treatment of wood samples to remove the lignin, increasing process complexity and carbon footprint, and no images were given for the ceria-based ecoceramics. In 2016 Pullar et al. [16] reported a more environmentally friendly approach to produce CeO_2 powder from waste cork sawdust, preserving the structure of the cork powder (200–500 μm grains) which was used as a template. These were the first reported pure-ceria ecoceramics, but only as a fine powder not suitable for TCFP or fuel cell applications. Recently, the use of ceria ecoceramics as redox material to promote CO_2 spilling using concentrated solar energy has been reported [17]. However, this study was focused on the catalysts (cork-ecoceramics and ceria foams ceramics prepared using polymeric templates) performance and did not address the ceria ecoceramics production. In the current paper we report for the first time the synthesis of 3DOM CeO_2 monoliths (cm size) from solid cork bark, and investigate the effects of different processing methods on the biomimetic cork microstructure. The impregnation of bulk cork samples, as reported here, is not a trivial matter due to the hydrophobic nature of cork and to its closed pore structure. Indeed the impregnation technique previously reported for cork powder [16] cannot be used for bulk cork impregnation. For the first time two approaches for impregnating the bulk cork samples, using multiple liquid infiltrations at low pressure, and infiltration under high pressure were evaluated. For this reason, the present investigation is a significant and necessary step forward in comparison with previous investigations considering the production of CeO_2 ecoceramics [16,33], as bulk forms are necessary for many key applications such as TCFP or fuel cells.

In the present work, the microstructure of these cork-derived CeO_2 ecoceramics is studied as a function of infiltration technique (use of low or high pressure), number of infiltration cycles and sintering temperature. Highly porous and lightweight 3DOM CeO_2 bulk ceramics were produced preserving the cellular structure of cork, which may allow their use for thermochemical fuel production using concentrated solar energy. They were produced using sustainable cork as a template, through a simple and flexible procedure, completely aqueous based and using no solvents, acids or bases. This follows several of the principles of green chemistry [34]. These CeO_2 bulk monoliths can be easily handled and collected after synthesis or use. Furthermore, they were produced using a natural and sustainable template (cork), which is collected without damaging the trees, and any carbon dioxide released during cork pyrolysis will be neutralised by that absorbed by the tree during growth of the next generation of cork bark, greatly reducing the carbon footprint of the process.

2. Experimental

2.1. Synthesis

Bulk cork samples were supplied by Amorim, and then used as-received. These cork specimens had been immersed in hot water (100 °C), which is a typical treatment performed on cork before its use to expand the cork cells, creating a more regular and uniform cell structure [23], and it is known as boiled cork.

The as-received cork samples were placed in graphite crucibles and then pyrolysed under nitrogen in a graphite furnace according to the following cycle: (i) 5 °C/min heating rate up to 150 °C; (ii) 10 °C/min heating rate up to 900 °C; 30 min dwell time at this temperature; and (iv) cooling (at 10 °C/min) to room temperature.

A cerium nitrate solution ($Ce(NO_3)_3.6H_2O$, 99%, Sigma Aldrich) was used to impregnate the pyrolysed cork specimens. The amount of carbon in the pyrolysed cork was estimated from its weight, and then an aqueous solution containing the equivalent number of moles of cerium was used. The impregnation was performed using two different methods to evaluate the influence of pressure on the infiltration efficiency:

i using a rotary evaporator under vacuum (55 °C and 60 mbar (6000 Pa) pressure); and
ii using an isostatic press (20 MPa and 30 s pressing time).

In both methods, multiple infiltrations (up to four cycles) were performed to evaluate their influence on the infiltration progress, and on the subsequent microstructure of the CeO_2 ecoceramics produced.

After infiltration, samples were dried at 80 °C for 12 h, and then heated in air to 1000 or to 1600 °C (1 °C/min heating rate; 30 min dwell time at maximum temperature) to produce porous ceria ecoceramics. The schematic representation of the procedure used for the CeO_2 synthesis is illustrated in Fig. 1.

2.2. Materials characterisation

The crystal structure of the ecoceramics was assessed by X-ray diffraction (XRD), using a PANalytical X'PERT PRO 3 instrument (Cu Kα radiation, 5–80°, 0.01° 2θ step-scan and 200 s/step), and phase identification by HighScore Plus software.

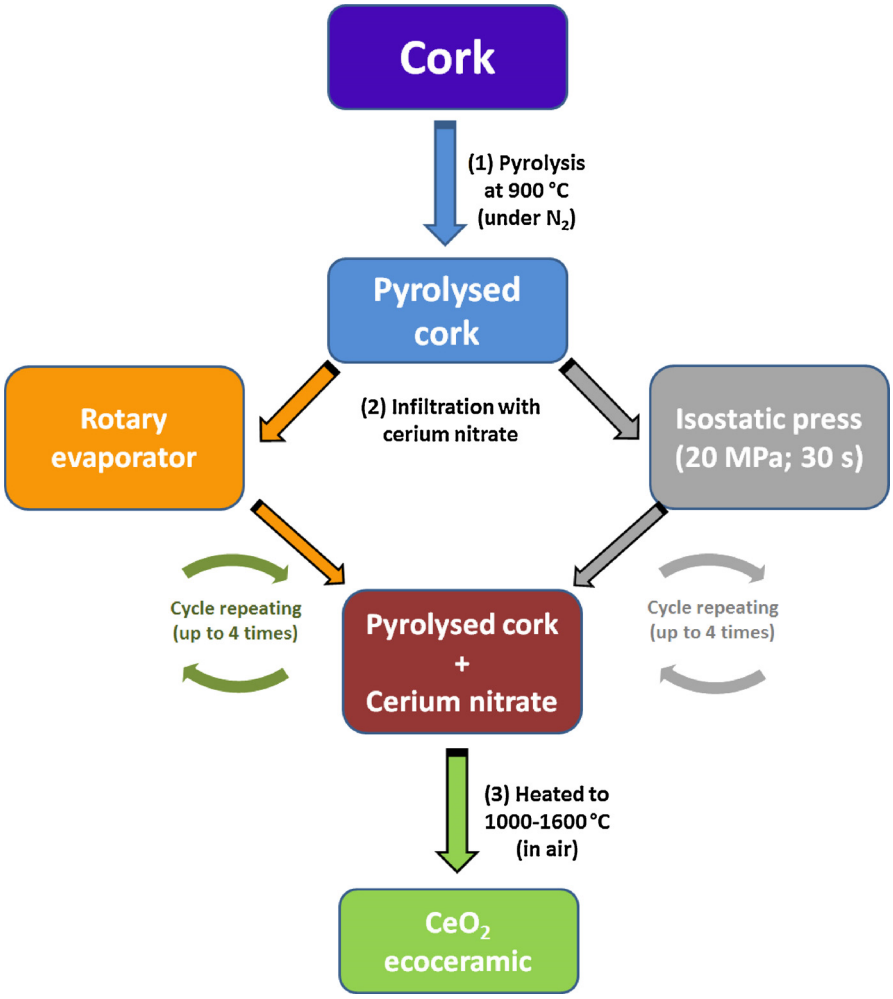

Fig. 1. Schematic representation of the procedure used for the CeO_2 ecoceramic synthesis using cork as template.

Scanning electron microscopy (SEM - Hitachi S4100 equipped with energy dispersion spectroscopy, EDS – Rontec) was used, at 25 kV, to investigate the microstructure of the cork templates and the eco-ceramics, after coating with carbon when necessary.

Simultaneous thermogravimetic–differential scanning calorimetry (TG-DSC) was performed using a Setsys Evolution 1750 (Setaram), with samples being heated at 10 °C/min under air or nitrogen.

The bulk density of cork, pyrolysed cork and that of the CeO_2 eco-ceramics was measured by the geometric method. For comparison the bulk density of CeO_2 discs, prepared using commercial powder (Cerium (IV) oxide, 99.5%, Alfa Aesar), was also measured. The CeO_2 powder was dry-pressed into discs using a stainless steel die (10 mm diameter). The discs were dried (80 °C for 12 h) and then heated in air to 1600 °C (1 °C/min heating rate; 30 min dwell time at maximum temperature).

3. Results and discussion

3.1. Cork and pyrolysed cork characterisation

Fig. 2 presents a photograph of the cork before and after pyrolysis, while the apparent density, mass and volume changes occurring during pyrolysis are provided in Table 1. The pyrolysis induces significant weight reduction (72%) and volume expansion (~34%). In fact, a nearly 5-fold decrease in apparent density was observed for the pyrolysed cork in comparison with the as-received cork, from 0.163 to only 0.034 g/cm^3.

Fig. 3 shows the TG-DSC curves of cork, pyrolysed cork and

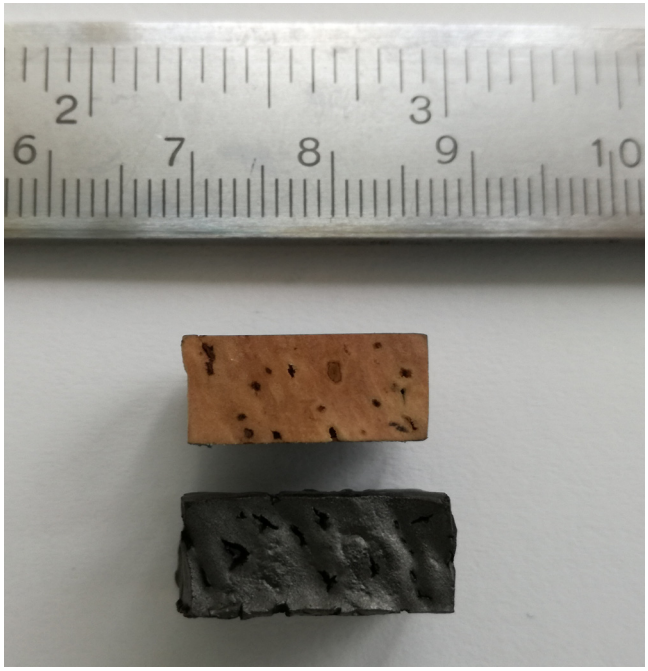

Fig. 2. Photograph of boiled cork before (top) and after (bottom) pyrolysis.

Table 1
Apparent density, mass and volume changes after cork pyrolysis.

Template	Density before pyrolysis (g/cm^3)	Density after pyrolysis (g/cm^3)	Mass residue (%)	Volume residue (%)
Boiled cork	0.163 ± 0.010	0.034 ± 0.001	28.0	134.3 ± 12.6

pyrolysed cork infiltrated with a cerium nitrate solution in distinct atmospheres (air and nitrogen). In air, cork shows three different weight losses: i) around 1.5% between room temperature and 100 °C, corresponding to the removal of physically adsorbed water from the cork, connected to the endothermic peak seen in Fig. 3b; ii) about 64% between 100–450 °C, due to the organic matter decomposition, associated with the two exothermic peaks (see Fig. 3b); and iii) around 34.5% up to 550 °C which is attributed to the decomposition of the remaining carbon and hydrocarbons. The observed stepwise decomposition pattern is common in lignocellulosic materials [35,36]. Cork is thermally stable up to 200 °C, and then decomposition increases with temperature and time, as hemicelluloses degrade in the initial steps, with suberin and lignin showing greater thermal resistance [36]. These results are in line with other thermogravimetric studies performed on cork [13,36]. The TG curve for the pyrolysed cork (in air) differs from that observed for the as-received cork. The weight loss between 100–450 °C is ~8%, significantly lower than that of cork, and attributed to the absence of volatile compounds which were converted to carbon during pyrolysis. Afterwards, a significant weight loss (~82%) up to 580 °C is shown, suggesting that the decomposition of the carbon structure it completed by this temperature, thus explaining the exothermic peak observed between 450 and 580 °C. The TG-DSC curve of the pyrolysed cork infiltrated with the ceramic precursor, presented in Fig. 3c, shows three different features: i) an endothermic peak at temperatures below 100 °C connected with the water release from the specimen, corresponding to a weight loss of ~24%; ii) a ~34% weight loss between 100 and 250 °C, attributed to the decomposition of $Ce(NO_3)_3$ into CeO_2 and oxides of nitrogen; and iii) a highly exothermic reaction is observed between 500 and 600 °C due to the abovementioned decomposition of the carbon structure, in this case corresponding to a ~13% weight loss. A comparison between the weight losses of the three studied systems is shown in Fig. 3d, further illustrating the thermal decomposition differences between them.

In nitrogen, some differences are perceived between the studied samples. Cork shows a similar thermal decomposition up to 500 °C in comparison with that shown when using an oxidative atmosphere. However, the heat transfer associated with cork pyrolysis (nitrogen) is substantially smaller than that observed when cork is heated in air (see Fig. 3b). Moreover, using an inert atmosphere generated an ash residue of around 14%. As for the pyrolysed cork, no significant features are observed in the curves, showing that further pyrolysis cycles are not relevant.

SEM micrographs of the cork are shown in Fig. 4a-c. The typical microstructure consists of ~20 μm hexagonal cells in the radial direction, and 40–50 μm long rectangular cells in the tangential or axial section, as is visible in Fig. 4a and 4b, respectively. A high magnification micrograph of the cell walls is provided in Fig. 4c, and they have a thickness of between 750–900 nm. After pyrolysis, the general microstructure (cell dimensions and shapes) was preserved, as is clearly demonstrated by the micrographs shown in Fig. 4 d–e. However, some of the hexagonal rear cell walls have opened due to pyrolysis, as shown with a sizeable hole being visible in Fig. 4e. This can be particularly important as it will increase open porosity compared to the unpyrolysed cork, and may enable the production of porous 3DOM CeO_2 with high surface area. Fig. 4f shows that although the cell dimensions have remained the same, the thickness of the cell walls has decreased greatly in the pyrolysed cork, to around half of their original thickness.

3.2. CeO_2 ecoceramics characterisation

3.2.1. Microstructural and XRD analysis

SEM micrographs of the CeO_2 ecoceramics infiltrated at low pressure on the rotary evaporator (method i)), after firing at 1000 °C in air, are presented in Fig. 5 (see top line). The micrographs show that the microstructure of the CeO_2 ecoceramics is similar to that of cork. Indeed, hollow hexagonal honeycomb cells are clearly observed.

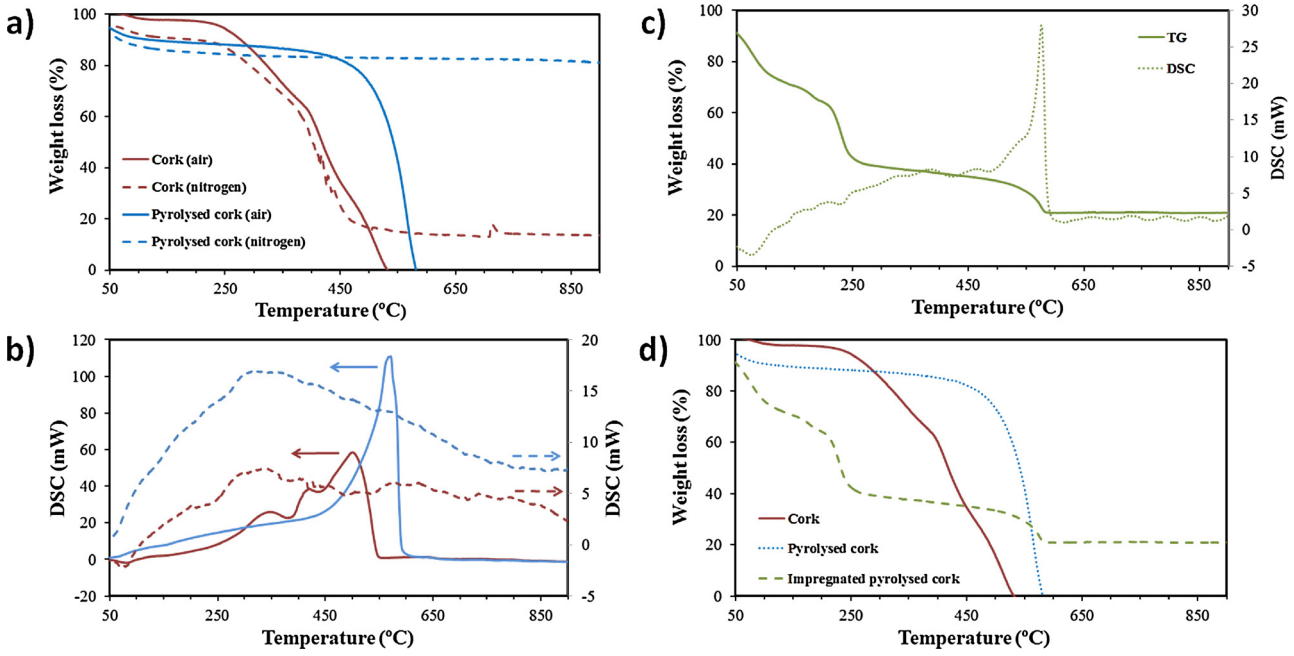

Fig. 3. a) TGA and b) DSC curves of cork before and after pyrolysis, in both air and nitrogen atmospheres. c) TGA and DSC pyrolysed cork infiltrated with a cerium nitrate solution in air. A comparison between the different systems is shown in d). Note: In Fig. 3b there are two y-axes, on two different scales. The solid lines (cork and pyrolysed cork in air) should be read on the left-hand axis, while the dashed lines (cork and pyrolysed cork in nitrogen) should be read on the right-hand axis, as indicated by the arrows.

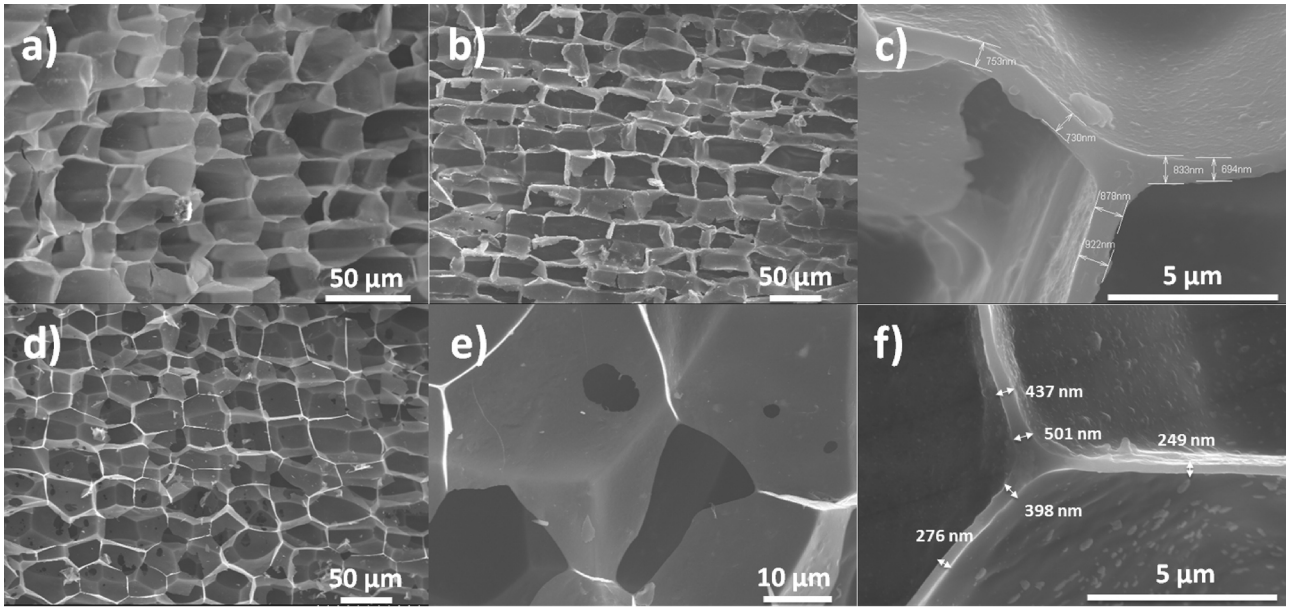

Fig. 4. SEM micrographs of cork before (a–c) and after pyrolysis (d–f).

However, one very important difference is that many of the cell walls are pierced, which is advantageous for applications where gases or fluids are intended to permeate into the structure. This feature will be particularly relevant in thermochemical fuel production, due to the expected increase in open porosity and available surface area.

The XRD pattern of the ceria ecoceramics (method i)) heated to 1000 °C, presented in Fig. 6, shows that this material consists of highly crystalline single phase CeO_2. It has the cubic fluorite structure (Fm3m), matching JCPDF standard no. 00-34-0394. All of the ceria ecoceramics investigated here showed similar, single phase XRD patterns.

3.2.2. *Influence of infiltration cycles*

The variation in weight gain of the pyrolysed cork samples infiltrated under low pressure (method i)) with cerium nitrate solution for between one and four infiltration/drying cycles was measured, and the results are presented in Fig. 7. The weight gain of the specimens after using the high pressure method (method ii)) was also included in the figure, and will be discussed in the next section (*3.2.3*).

The first infiltration resulted in a significant increase in mass (~660%). The accumulated mass further increases with subsequent cycles, reaching a maximum of ~1200% after the fourth infiltration. However, the rate of increase in weight is steadily diminishing with subsequent infiltrations, suggesting that a plateau is being reached at this stage, and indeed we found that repeating up to seven infiltration cycles had little effect beyond that achieved with the fourth. With four infiltrations, the pyrolysed cork was able to absorb up to 12 times its initial weight of cerium nitrate. This is due to both the higher surface area induced by pyrolysis from the loss of some cell walls, and the high degree of mesoporosity observed in pyrolysed wood samples, with pores between 2–10 nm [33]. By contrast, untreated cork contains mostly closed cells, which are responsible for its low water and air

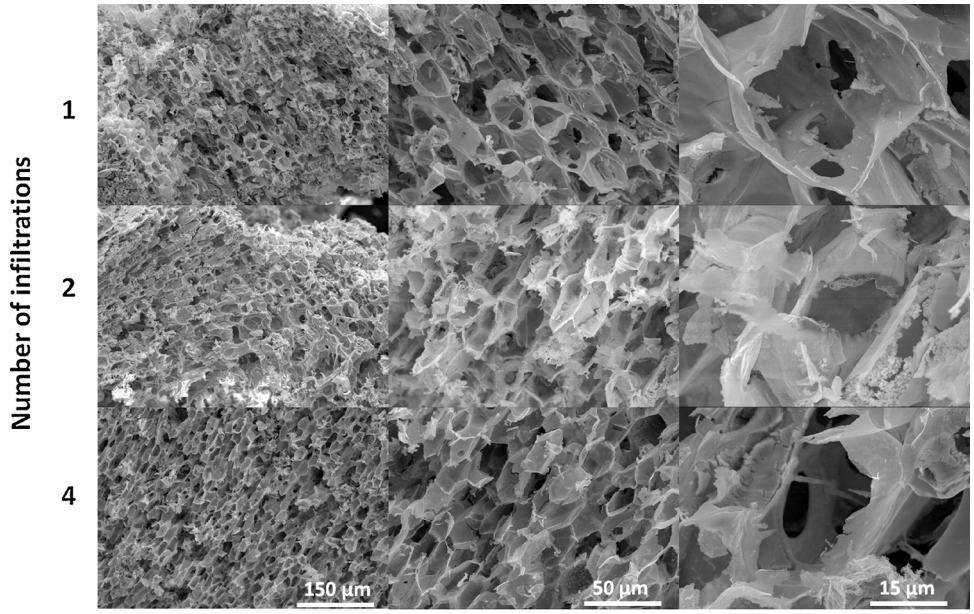

Fig. 5. SEM micrographs of CeO_2 ecoceramics (fired to 1000 °C) produced using cork as a template, infiltrated 1, 2 and 4 times under low pressure with cerium nitrate solution.

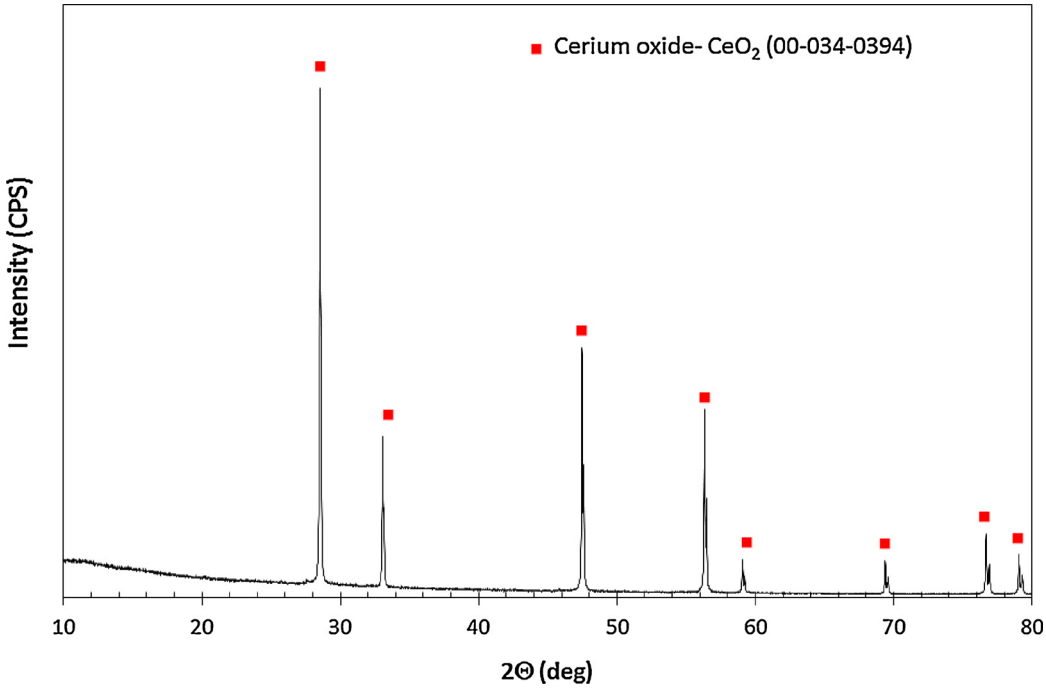

Fig. 6. XRD pattern of the CeO_2 ecoceramics (fired to 1000 °C) produced using cork as template, produced using method i).

permeability [23]. After firing the specimens submitted to 4 infiltration cycles lose 59.9 ± 1.1% of their weight, which was associated both with water release and nitrates combustion as shown by the TG-DSC curves (see Fig. 3c).

The microstructural changes of the CeO_2 ecoceramics promoted by multiple infiltrations are illustrated in the SEM micrographs shown in Fig. 5. After the first infiltration followed by heating to 1000 °C, CeO_2 ecoceramics with hexagonal cells mimicking cork structure were produced. As the number of infiltrations rises, the amount of cerium nitrate deposited on the pyrolysed cork cells increases, filling (partially or completely) some of the cells. After firing, the CeO_2 ecoceramics infiltrated two times or four times show lower porosity than their single infiltration counterparts. Indeed, several filled hexagonal cells are observed in the SEM micrographs after 4 cycles of infiltration (see inset micrographs in Fig. 7). In line with these remarks, we also observed that the mechanical stability of the specimens was higher for the samples that underwent a greater number of infiltrations. Considering the higher mechanical stability of the samples infiltrated 4 times with cerium nitrate, they were selected to evaluate the influence of sintering temperature on the ecoceramics' microstructure (discussed in section *3.2.4*). It should also be highlighted that despite the increase in mechanical stability (fired at 1000 °C) as the number of infiltration cycles increases, their strength is significantly lower than those sintered at higher temperature (see section *3.2.4*).

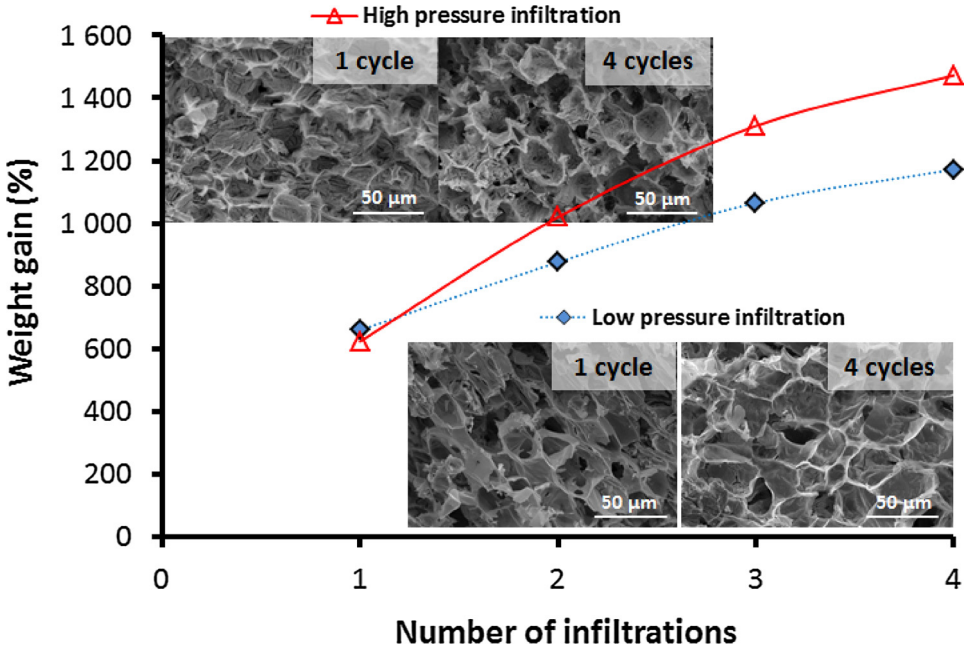

Fig. 7. Weight gain of the pyrolysed cork after consecutive infiltrations with cerium nitrate solution under low (method i)) and high pressure (method ii)). The inset SEM micrographs illustrate the subsequent CeO_2 microstructure after firing to 1000 °C.

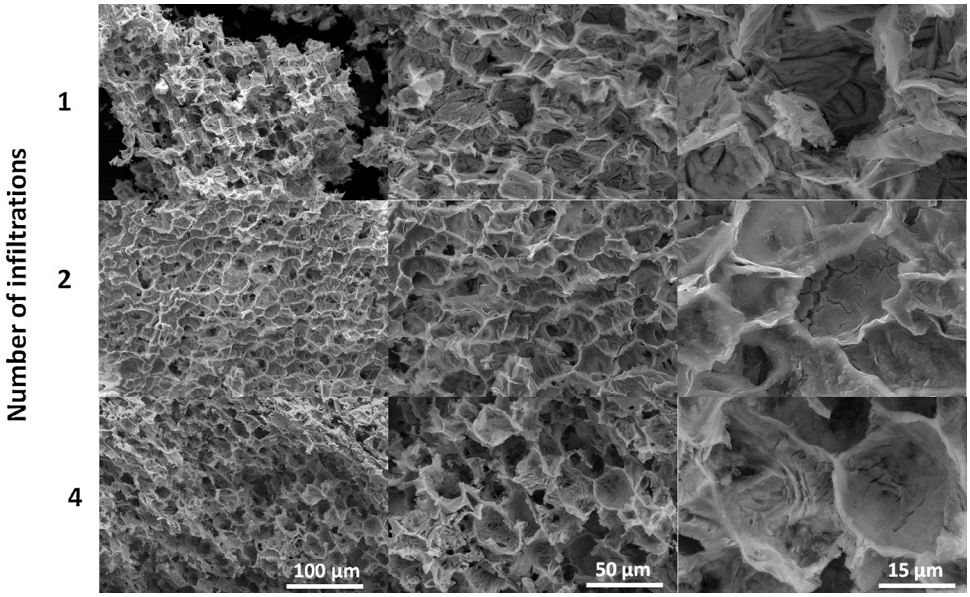

Fig. 8. SEM micrographs of CeO_2 ecoceramics (fired to 1000 °C) produced using pyrolysed cork as a template, infiltrated 1, 2 and 4 times with cerium nitrate solution at high pressure (20 MPa).

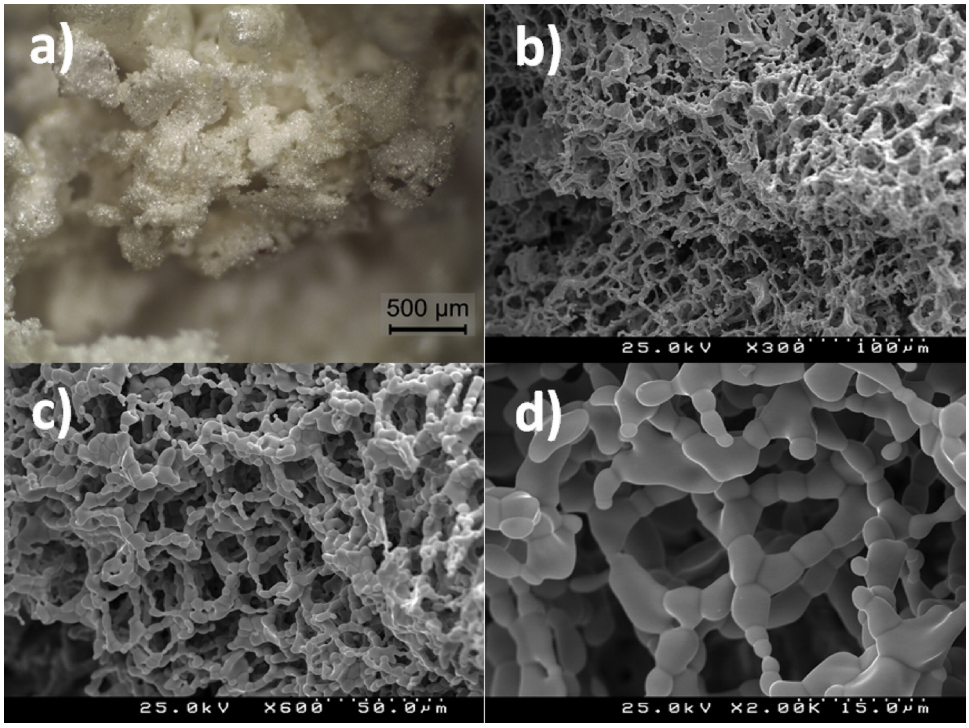

Fig. 9. a) Optical photograph and (b–d) SEM micrographs of CeO_2 ecoceramics (produced using pyrolysed cork infiltrated 4 times with cerium nitrate solution under low pressure) heated to 1600 °C.

3.2.3. Influence of infiltration technique

To compare with the low pressure infiltration of method i), pyrolysed cork specimens were also infiltrated with cerium nitrate solution under high pressure using an isostatic press, as described in method ii). Fig. 7 shows that, despite the higher pressure of method ii) in comparison with method i), a similar weight gain was obtained after the first infiltration/drying cycle. This feature is attributed to the shorter infiltration time (30 s) used here in comparison with that of the vacuum infiltration technique (method i)), where the pyrolysed cork was in contact with the cerium nitrate solution for ~ 30 min. Nevertheless, after the second infiltration the high pressure method is more effective than the low pressure technique, an increase in the weight gain of around 140% being observed. The weight gain difference between the two methods further increases after the 4th infiltration/drying cycle, reaching 300%, meaning that at this point the pyrolysed cork absorbs 15 times its initial weight in cerium nitrate when applying high pressure and 12 times when using the low pressure method.

The microstructure of the CeO_2 ecoceramics produced by method ii), and with multiple infiltrations, is shown in Fig. 8. Once again, the initial cork structure was replicated in the CeO_2, with clear hexagonal cells being distinguished in the micrographs. However, there is a substantial difference in the cell wall morphology of these ecoceramics in

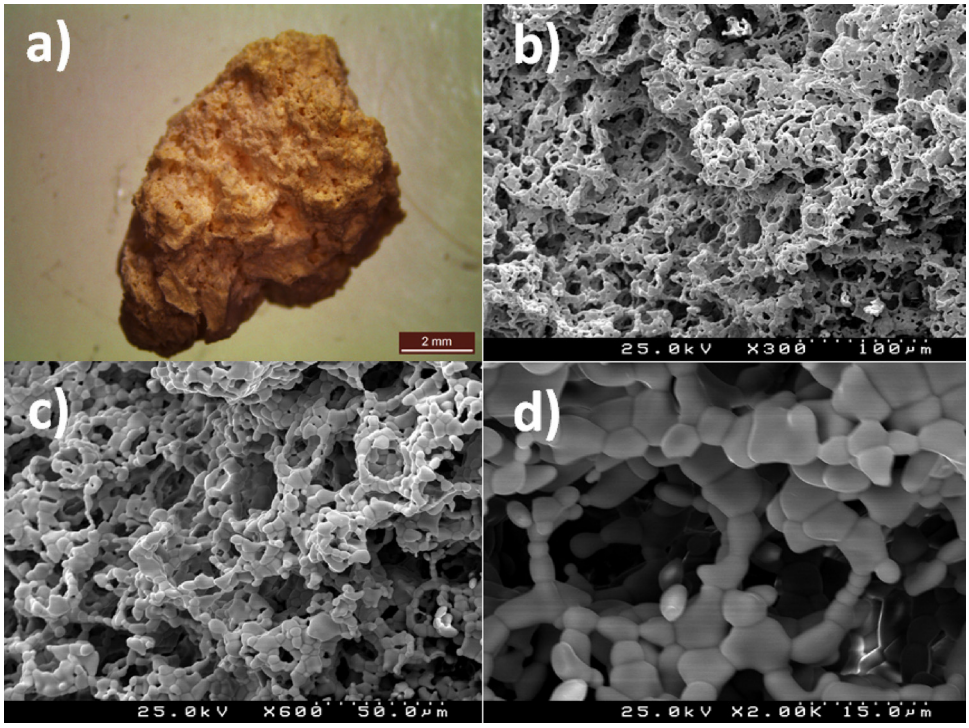

Fig. 10. a) Optical photograph and (b–d) SEM micrographs of CeO_2 ecoceramics infiltrated one time with cerium nitrate solution at high pressure (20 MPa) and then heated to 1600 °C.

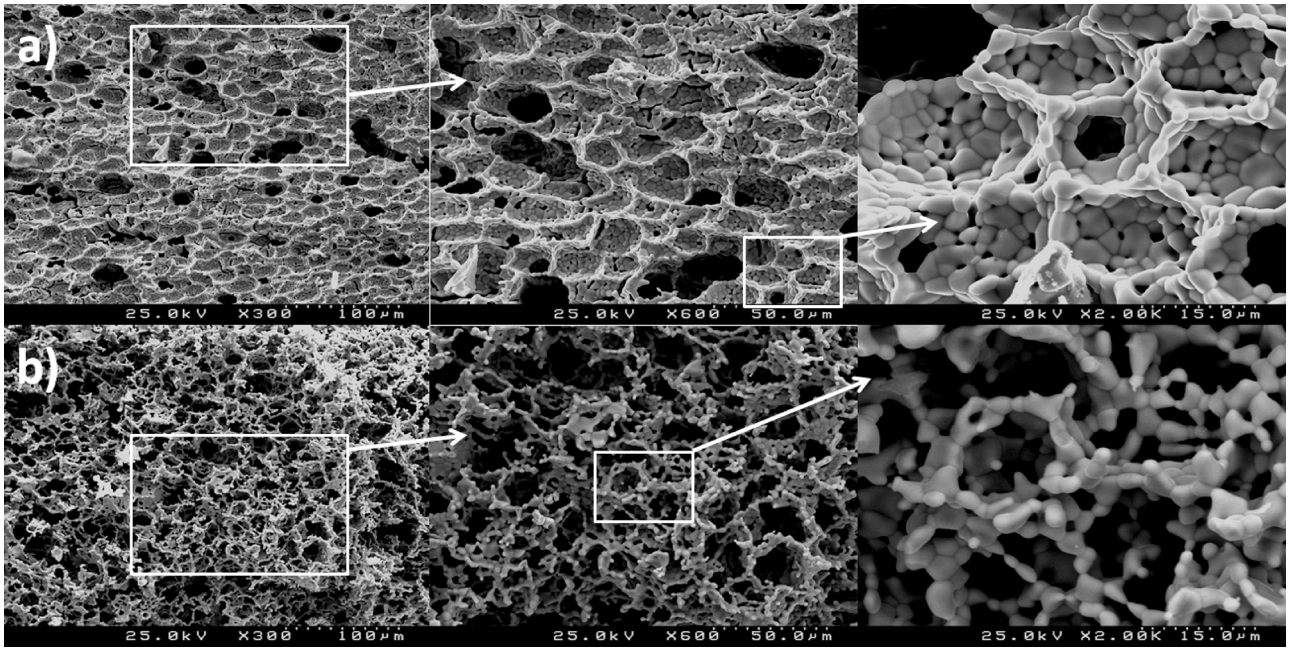

Fig. 11. SEM micrographs at two different plots of CeO_2 ecoceramics infiltrated four times with cerium nitrate solution at high pressure (20 MPa) and then heated to 1600 °C.

comparison with those prepared at low pressure (method i), 60 mbar using a rotary evaporator), and after 20 MPa pressure was applied, the cell walls show several cracks, suggesting that the cork structure was damaged during the process. These cracks are particularly visible in the specimens subjected to one infiltration cycle (see top SEM micrographs in Fig. 8). The use of a higher number of infiltrations (between 2 and up to 4) enhances the specimens' mechanical stability, similar to that observed when using the low infiltration regime.

The comparison between the ceria microstructure achieved with the two infiltration regimes (see Figs. 5 and 8), as well as the specimens' weight gain with multiple infiltrations (see Fig. 6), suggests that a denser microstructure is produced when using the high pressure method, comparing equal numbers of infiltration/drying cycles. For this reason, two specimens were selected for the next section (*3.2.4* - Influence of sintering temperature): samples submitted to 1 and 4 infiltration cycles.

3.2.4. Influence of sintering temperature

a) Samples prepared with the low pressure regime (method i))

Fig. 9 shows optical and SEM micrographs of CeO_2 produced after heating the impregnated samples to 1600 °C. The higher sintering temperature promoted significant grain growth in comparison with the samples fired at 1000 °C: from ~100 nm [16] to several μm. The latter is in agreement with previous studies where grain growth of CeO_2 was observed when temperature increased [32].

Even though the grain size increases, the ceria ecoceramics are still highly porous as demonstrated by the SEM micrograph shown in Fig. 9b, and the hexagonal 3DOM cork structure is preserved. Moreover, the larger grain sizes allowed the production of stable, highly porous cm-sized CeO_2 monoliths, as demonstrated in the optical micrograph in Fig. 9. In fact, these samples showed much higher mechanical stability in comparison with their lower firing temperature counterparts (see section 3.2.2) and therefore can be easily handled.

With the increase in grain size to several microns, the side walls of the cells forming the hexagonal structure have increased greatly in thickness, and this appears to have resulted in migration of materials from the rear walls of the cells, creating a completely open porous structure. Despite this increase in wall thickness, however, the diameter of the hexagonal cells has remained constant, at ~20 μm, retaining the 3DOM cork structure. This is the first ever report of bulk CeO_2 ecoceramic monoliths (cm size) produced using any kind of wood as a template.

To further characterize the CeO_2 ecoceramics the bulk density of the specimens fired at 1600 °C infiltrated at low pressure (shown in Fig. 9) was determined and compared with that of CeO_2 discs sintered at 1600 °C from commercial ceria powder. The bulk density of the CeO_2 discs was 6.7 g/cm^3, corresponding to ~92% of the theoretical density of ceria. As for the ecoceramics their apparent density was 0.41 g/cm^3. The density of these ceria ecoceramics is 16 times lower than that observed for the disc produced with commercial powder. The total porosity of these specimens reached a striking ~ 94%, which is in line with the SEM micrographs presented in Fig. 9 that show an open porous structure.

- Samples prepared with the high pressure regime (method ii))

Figs. 10 and 11 present SEM micrographs of the ceria ecoceramics produced using pyrolysed cork infiltrated one and four times with cerium nitrate solution, respectively. Both strategies (one or four infiltration cycles) allowed the production of cm size specimens; however, the ecoceramics' microstructure, bulk density and total porosity is modified. The use of one infiltration cycle leads to the production of highly porous ecoceramics with homogeneous microstructure. The sample submitted to four infiltration cycles also presents a microstructure mimicking that of the cork template (see Fig. 11), but it is heterogeneous: part of the specimen is highly porous (see Fig. 1b), while other parts show lower porosity (see Fig. 11b). This was attributed to the greater amount of ceria deposited on the pyrolysed cork cells as a consequence of the higher number of infiltration cycles, as demonstrated by the weight gain presented in Fig. 5. The amount of cerium nitrate infiltrated into the pyrolysed cork was also found to affect the CeO_2 apparent density: 0.67 and 0.84 g/cm^3 for the specimens infiltrated one and four times, respectively. The density here achieved is 8 (four infiltration cycles) to 10 (one infiltration cycle) times lower than that of the sintered discs produced with commercial powder. It is also between 1.7–2.1 times higher than that reached using the low infiltration regime (0.41 g/cm^3). In line with these results, the specimens also show lower total porosity 88.7% (one infiltration cycle) and 90.7% (four infiltration cycles) in comparison with that produced with the low infiltration regime (94.4%). These results show that despite promoting higher infiltration levels (see Fig. 7), the high pressure regime led to the production of lower porosity ecoceramics (88.7% instead of 94.4%; comparing the same number of infiltration cycles). Nevertheless, results also show the possibility of tailoring the porosity of the ecoceramics and, therefore, their specific surface area, simply by modifying the number of infiltration cycles. This may allow the production of ecoceramics with various porosities for distinct catalytic applications.

Both impregnation strategies (low and high pressure) resulted in the production of porous CeO_2 monoliths. However, the infiltration efficiency and the number of infiltration cycles were found to strongly affect the ecoceramics' microstructure. In any case, the higher porosity (between 3.3 and 5.7%) achieved when using the low pressure method suggests the better suitability of this strategy to produce highly porous CeO_2 catalysts. Indeed, the higher porosity may allow higher gas permeability through the ecoceramic and, therefore, a greater reactive surface, which could be advantageous for certain applications (e.g. TCFP). The exceptional 3DOM porous structure exhibited by these CeO_2 ecoceramic monoliths may allow their use in the thermochemical fuel production, and this topic will be addressed in future work. This possibility has been recently demonstrated by the authors using polymer templated (cm size) and cork-based CeO_2 foams (mm size) [17].

4. Conclusions

Cork is harvested without damaging the tree, thus making it an exceptional sustainable material. Moreover, its regular 3DOM structure consisting of hollow hexagonal honeycomb cells makes it an ideal template for the production of ecoceramics. This investigation evaluates for the first time the influence of the infiltration regime, number of infiltration cycles and sintering temperature on the microstructure of the ceria monolith ecoceramics (cm size).

Results show the possibility of tailoring the microstructure of the produced 3DOM CeO_2 ecoceramics by changing the number of infiltrations, the infiltration regime and sintering temperature.

Moreover, the infiltration technique was found to affect the specimens' total porosity, higher values reached when using lower infiltration pressure. Results show that the use of higher sintering temperature (1600 °C) combined with lower infiltration pressure led to the production of highly porous (94.4%) but mechanically stable specimens, which decreases the existing knowledge gap regarding porous ceria ecoceramics production and may contribute towards its use in catalytic applications.

Data availability

The raw/processed data required to reproduce these findings cannot be shared at this time due to legal or ethical reasons.

Acknowledgements

R.C. Pullar wishes to thank FCT grant IF/00681/2015 for supporting this work, and R.M. Novais wishes to thank FCT project H2CORK (PTDC/CTM-ENE/6762/2014). The authors acknowledge Amorim Cork Composites for providing the cork samples. This work was developed within the scope of the project CICECO-Aveiro Institute of Materials, POCI-01-0145-FEDER-007679 (FCT Ref. UID/CTM /50011/2013), financed by national funds through the FCT/MEC and when appropriate co-financed by FEDER under the PT2020 Partnership Agreement.

References

[1] M. Singh, J. Martínez-Fernández, A.R. de Arellano-López, Environmentally conscious ceramics (ecoceramics) from natural wood precursors, Curr. Opin. Solid State Mater. Sci. 7 (2003) 247–254.
[2] M. Singh, B.-M. Yee, Reactive processing of environmentally conscious, biomorphic

ceramics from natural wood precursors, J. Eur. Ceram. Soc. 24 (2004) 209–217.
[3] J. Li, S. Yu, M. Ge, X. Wei, Y. Qian, Y. Zhou, W. Zhang, Fabrication and characterization of biomorphic cellular C/SiC-ZrC composite ceramics from wood, Ceram. Int. 41 (2015) 7853–7859.
[4] X. Kan, J. Ding, C. Yu, H. Zhu, C. Deng, G. Li, Low temperature fabrication of porous ZrC/C composite material from molten salts, Ceram. Int. 43 (2017) 6377–6384.
[5] M. Krzesińka, J. Zachariasz, The effect of pyrolysis temperature on the physical properties of monolithic carbons derived from solid iron bamboo, J. Anal. Appl. Pyrolysis 80 (2007) 209–215.
[6] G. Hou, Z. Jin, J. Qian, Effect of holding time on the basic properties of biomorphic SiC ceramic derived from beech wood, Mater. Sci. Eng. A 452-453 (2007) 278–283.
[7] Y. Shin, J. Liu, J.H. Chang, Z. Nie, G.J. Exarhos, Hierarchically ordered ceramics through surfactant templated sol-gel mineralization of biological cellular structures, Adv. Mater. 13 (2001) 728–732.
[8] P. Greil, T. Lifka, A. Kaindl, Biomorphic: cellular silicon carbide ceramics from wood: I Processing and microstructure, J. Eur. Ceram. Soc. 18 (1998) 1961–1973.
[9] T. Ota, M. Takahashi, T. Hibi, M. Ozawa, S. Suzuki, Y. Hikichi, H. Suzuki, Biomimetic process for producing SiC “wood”, J. Am. Ceram. Soc. 78 (1995) 3409–3411.
[10] H. Sieber, Biomimetic synthesis of ceramics and ceramic composites, Mater. Sci. Eng. A 412 (2005) 43–47.
[11] C.K. Sia, Y. Sasaki, N. Adachi, T. Ota, The magnetic properties of porous Ni–Zn ferrites prepared from wood templates, J. Ceram. Soc. Jpn. 117 (2009) 958–960.
[12] http://www.engineeringtoolbox.com/wood-density-d_40.html. Accessed May 2017.
[13] R.C. Pullar, P. Marques, J. Amaral, J.A. Labrincha, Magnetic wood-based biomorphic $Sr_3Co_2Fe_{24}O_{41}$ Z-type hexaferrite ecoceramics made from cork templates, Mater. Des. 82 (2015) 297–303.
[14] R.C. Pullar, R.M. Novais, Ecoceramics: cork-based biomimetric ceramic 3-DOM foams, Mater. Today 20 (2017) 45–46.
[15] V.O. Yukhymchuk, V.S. Kiselov, M. Ya, M.P. Valakh, M.A. Tryus, A.G. Skoryk, S.A. Rozhin, A.E. Kulinich, Belyaey, Biomorphous SiC ceramics prepared from cork oak as precursor, J. Phys. Chem. Solids 91 (2016) 145–151.
[16] R.C. Pullar, L. Gil, F.A.C. Oliveira, Biomimetic cork-based CeO_2 ecoceramics for hydrogen generation using concentrated solar energy, Ciâªncia Tecnol. Dos Mater. 28 (2016) 23–28.
[17] F.A. Costa Oliveira, M.A. Barreiros, S. Abanades, A.P.F. Caetano, R.M. Novais, R.C. Pullar, Solar thermochemical CO_2 splitting using cork-templated ceria ecoceramics, J. CO2 Utilization 26 (2018) 552–563.
[18] APCOR, Yearbook 2016. Portuguese Cork Association (Portugal), Available from: (2016) https://www.apcor.pt/.
[19] A.M. Matos, S. Nunes, J. Sousa-Coutinho, Cork waste in cement based materials, Mater. Des. 85 (2015) 230–239.
[20] O. Anjos, C. Rodrigues, J. Morais, H. Pereira, Effect of density on the compression behavior of cork, Mater. Des. 53 (2014) 1089–1096.
[21] http://www.saomarcosdaserra.com/cork.php. Accessed May 2017.
[22] L. Gil, Cork: a strategic material, Front. Chem. 2 (2014) 1–2 article 16.
[23] E.M. Fernandes, V.M. Correlo, J.F. Mano, R.L. Reis, Cork-polymer biocomposites: mechanical, structural and thermal properties, Mater. Des. 82 (2015) 282–289.
[24] O. Anjos, H. Pereira, M.E. Rosa, Tensile properties of cork in the tangential direction: variation with quality, porosity, density and radial position in the cork plank, Mater. Des. 31 (2010) 2085–2090.
[25] S.P. Silva, M.A. Sabino, E.M. Fernandes, V.M. Correlo, L.F. Boesel, R.L. Reis, Cork: properties, capabilities and applications, Int. Mater. Rev. 53 (2008), https://doi.org/10.1179/174328008X353529 256–256.
[26] F. Rollin-Genetet, C. Seidel, E. Artells, M. Auffan, A. Thiéry, C. Vidaud, Redox reactivity of cerium oxide nanoparticles induces the formation of disulfide bridges in thiol-containing biomolecules, Chem. Res. Toxicol. 28 (2015) 2304–2312.
[27] H. Huang, J. Liu, P. Sun, S. Ye, B. Liu, Effects of Mn-doped ceria oxygen-storage material on oxidation activity of diesel soot, RSC Adv. 7 (2017) 7406–7412.
[28] R. Chockalingam, V.R.W. Amarakoon, H. Giesche, Alumina/cerium oxide nanocomposite electrolyte for solid oxide fuel cell applications, J. Eur. Ceram. Soc. 28 (2008) 959–963.
[29] N.I. Santha, M.T. Sebastian, P. Mohanan, N. McN, K. Alford, R.C. Sarma, S. Pullar, A. Kamba, P. Pashkin, J. Samukhina, Petzelt, Effect of doping on the dielectric properties of cerium oxide in the microwave and far-infrared frequency range, J. Am. Ceram. Soc. 87 (2004) 1233–1237.
[30] A. Saadat-Monfared, M. Mohseni, M. Tabatabaei, Polyurethane nanocomposite films containing nano-cerium oxide as UV absorber. Part 1. Static and dynamic light scattering, small angle neutron scattering and optical studies, Colloids Surf. A Physicochem. Eng. Asp. 408 (2012) 64–70.
[31] A.L. Gal, S. Abanades, N. Bion, T.Le Mercier, V. Harlé, Reactivity of doped ceria-based mixed oxides for solar thermochemical hydrogen generation via two-step water-splitting cycles, Energy Fuels 27 (2013) 6068–6078.
[32] C.D. Malonzo, R. M De Smith, S.G. Rudisill, N.D. Petkovich, J.H. Davidson, A. Stein, Wood-templated CeO_2 as active material for thermochemical CO production, J. Phys. Chem. C 118 (2014) 26172–26181.
[33] B. Matovic, S. Boskovic, Synthesis of oxide ecoceramics, Romanian J. Mater. 38 (2008) 329–334.
[34] P.T. Anastas, J.C. Warner, Green Chemistry: Theory and Practice, Oxford University Press, New York, 1998 p.30.
[35] R.M. Novais, M.P. Seabra, J.A. Labrincha, Wood waste incorporation for lightweight porcelain stoneware tiles with tailored thermal conductivity, J. Clean. Prod. 90 (2015) 66–72.
[36] A. Şen, J.V. den Bulcke, N. Defoirdt, J.V. Acker, H. Pereira, Thermal behavior of cork and cork components, Thermochim. Acta 582 (2014) 94–100.